Supporting Information

N Coupling with S-Coordinated Ru Nanoclusters for Highly Efficient Hydrogen Evolution in Alkaline Media

Cheng-Fei Li,[a] Jia-Wei Zhao,[a] Ling-Jie Xie,[a] Yu Wang,[a] Hai-Bo Tang,[a] Li-Rong Zheng[b],* and Gao-Ren Li[a],*

[a]*MOE Laboratory of Bioinorganic and Synthetic Chemistry, The Key Lab of Low-carbon Chemistry & Energy Conservation of Guangdong Province, School of Chemistry, Sun Yat-sen University, Guangzhou 510275, China*

[b]*Beijing Synchrotron Radiation Facility, Institute of High Energy Physics, Chinese Academy of Sciences, Beijing 100049, China*

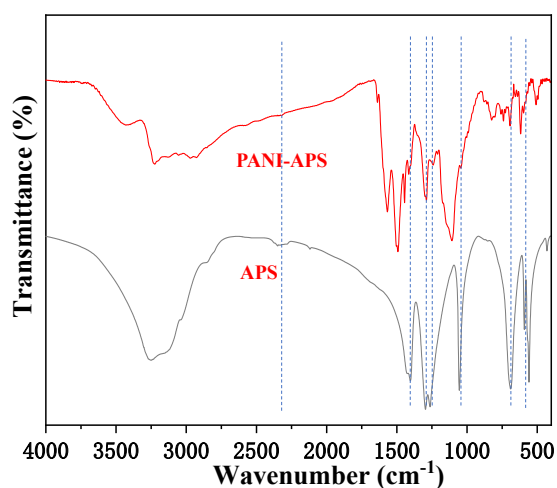E-mail: zhenglr@ihep.ac.cn; ligaoren@mail.sysu.edu.cn

Fig. S1 FT-IR spectra of PANI-APS (polyaniline-ammonia persulfate) and APS (ammonia persulfate) for reference.

Obviously, apart from these peaks at 1566, 1493, 1289, 1244, 1107 and 3434 cm^{-1} ascribed to C–C stretching of the quinonoid ring and benzenoid ring, C–N stretching of secondary aromatic amines, C–H bindings of the benzenoid ring and the quinonoid ring and N–H stretching in FT-IR spectrum of PANI-

APS, respectively, other partial bands are consistent with APS, indicating existence of the APS in the framework of PANI-APS.
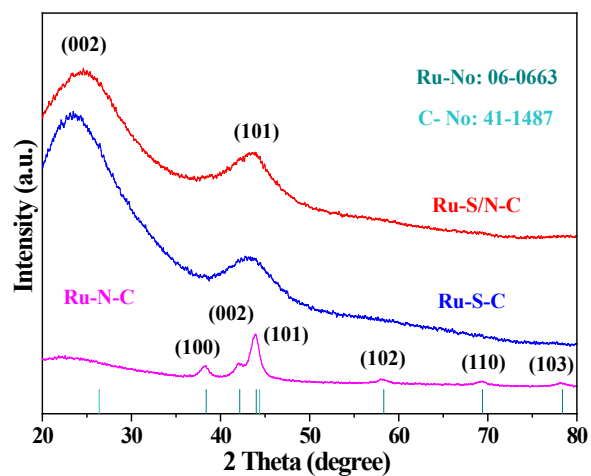

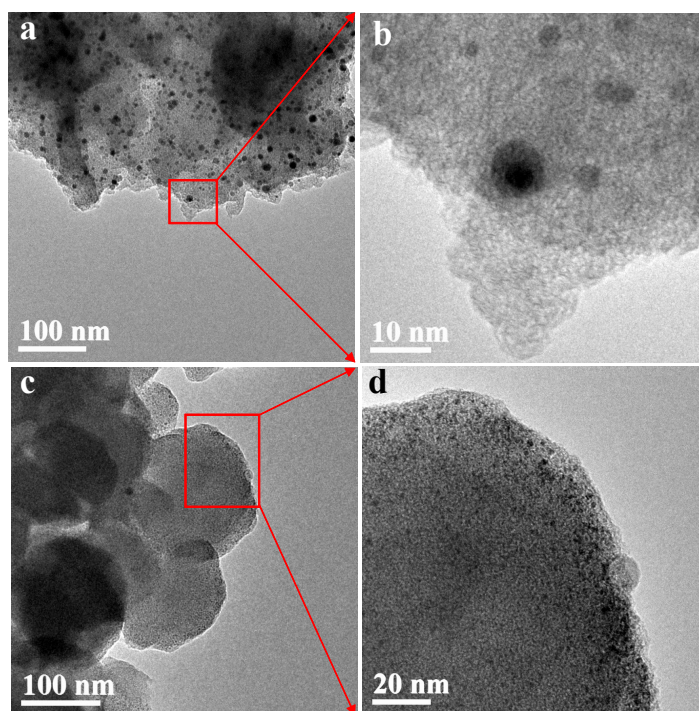**Fig. S2** XRD patterns of Ru-S/N-C, Ru-S-C and Ru-N-C.

Fig. S3 a) and b) TEM images of Ru-N-C with different magnifications; c) and d) TEM images of Ru-S-C with different magnifications.
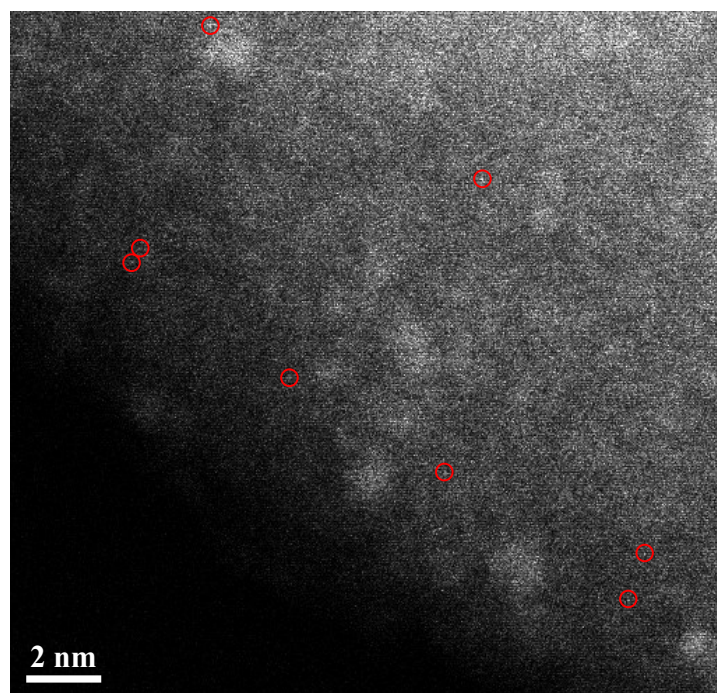
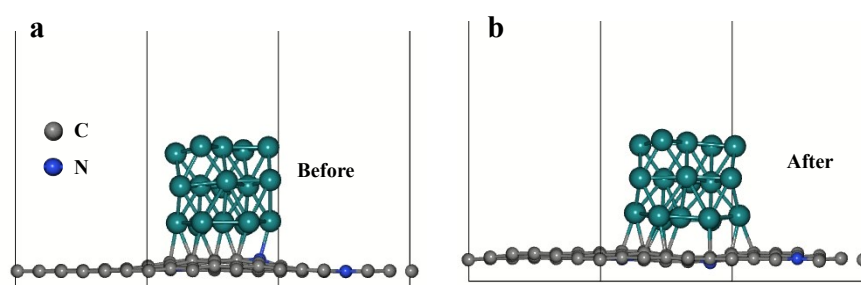**Fig. S4** The aberration-corrected HAADF-TEM of Ru-S/N-C. The Ru single-atoms were marked by the red circles.

Fig. S5 Theoretical models of Ru-N-C before (a) and after (b) structural optimization.
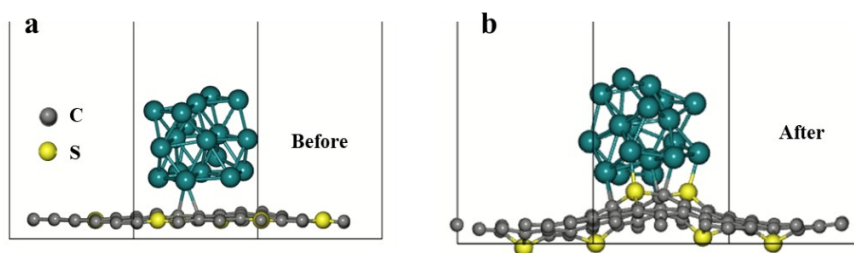

Fig. S6 Theoretical models of Ru-S-C before (a) and after (b) structural optimization.
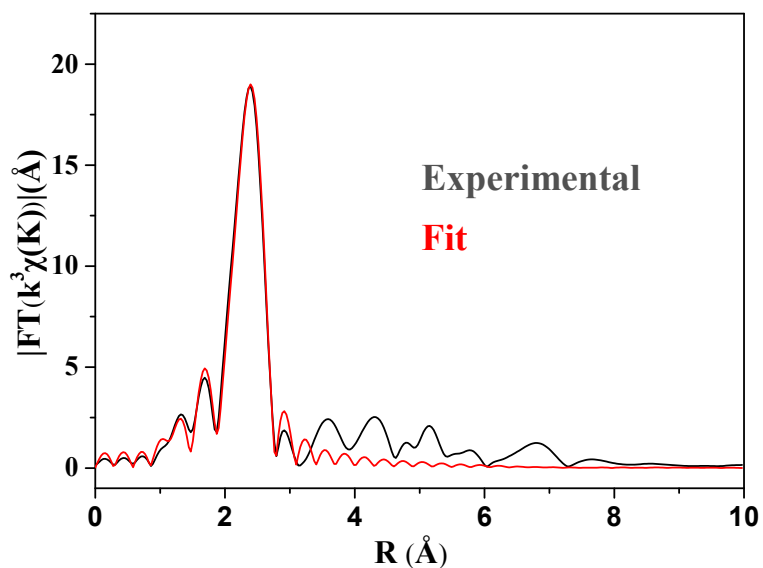
Fig. S7 FTEXAFS fitting curves of the Ru-S/N-C at Ru K-edge.

Table S1. EXAFS fitting parameters at the Ru K-edge for various samples

Sample	Shell	N [a]	R (Å) [b]	σ^2 (Å^2·10^{-3}) [c]	ΔE_0 (eV) [d]	R factor (%)
Ru-S/N-C	Ru-S	1.2±0.4	2.15±0.03	6.9±1.3	-7.3±0.8	0.7
	Ru-Ru	7.2±0.6	2.68±0.01	5.5±1.0	5.5±1.5	

[a] N: coordination numbers; [b] R: bond distance; [c] σ^2: Debye-Waller factors; [d] ΔE_0: the inner potential correction. R factor: goodness of fit. SO_2 were set as 0.815/0.823 for Ru-S/Ru-Ru, which were obtained from the experimental EXAFS fit of reference Ru powder/ RuS$_2$ by fixing CN as the known crystallographic value and was fixed to all the samples.
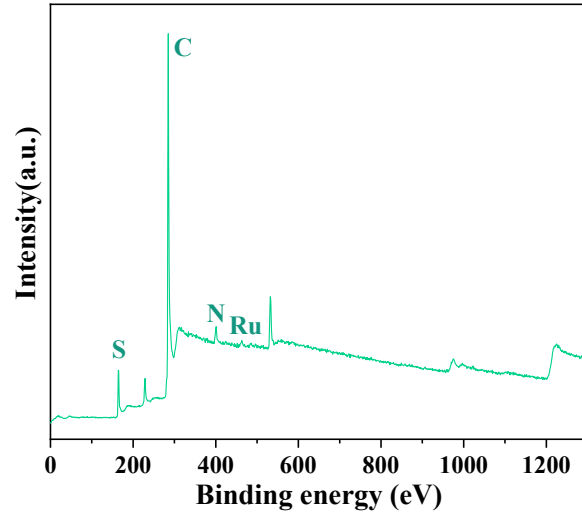
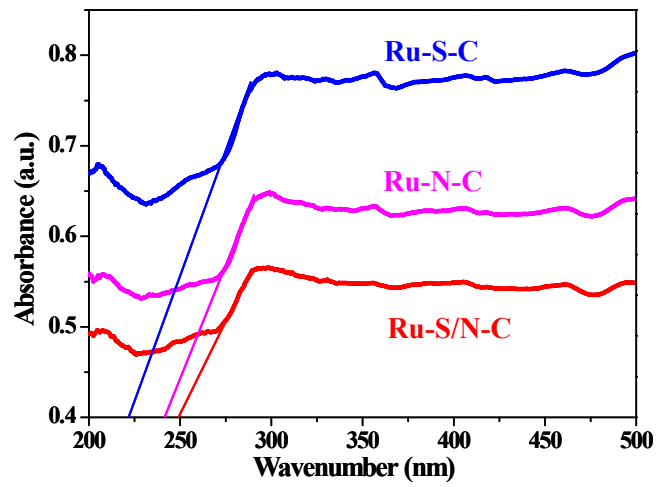**Fig. S8** The survey XPS pattern of Ru-S/N-C.

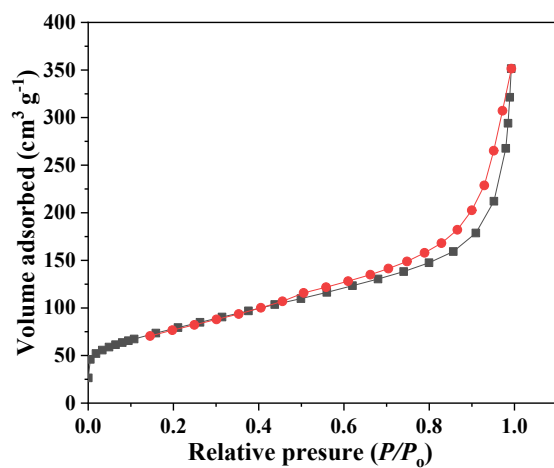**Fig. S9** UV-Vis diffuse reflectance spectra of Ru-S/N-C, Ru-N-C, and Ru-S-C.

Fig. S10 N$_2$ adsorption–desorption isotherms of Ru-S/N-C.
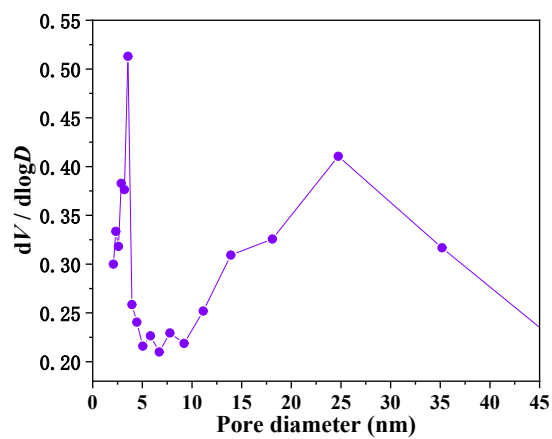

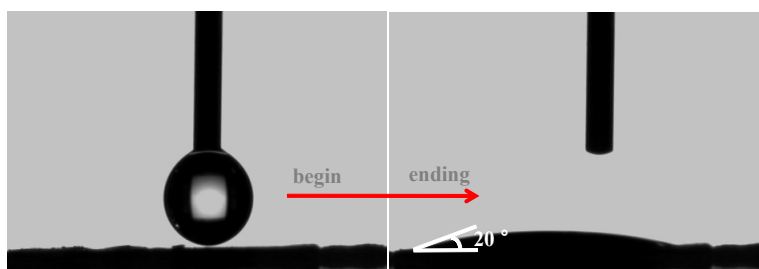**Fig. S11** Pore size distribution plot of Ru-S/N-C.
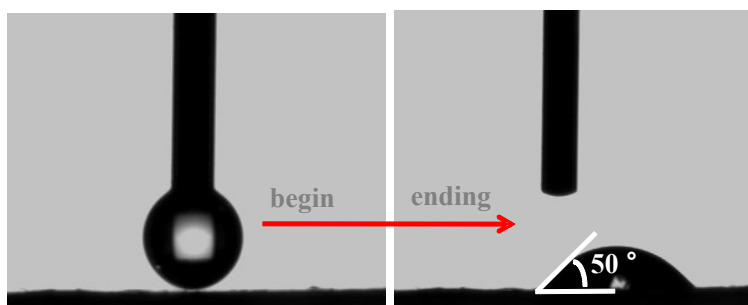
Fig. S12 The contact angle measurement of Ru-S/N-C.

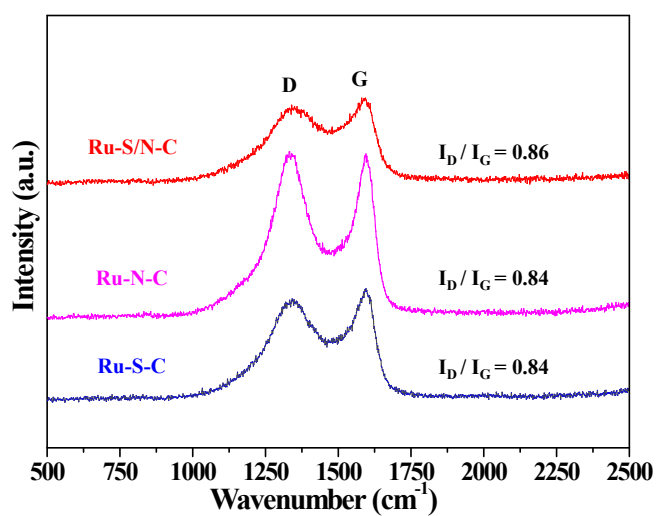**Fig. S13** The contact angle measurement of Ru-S-C.

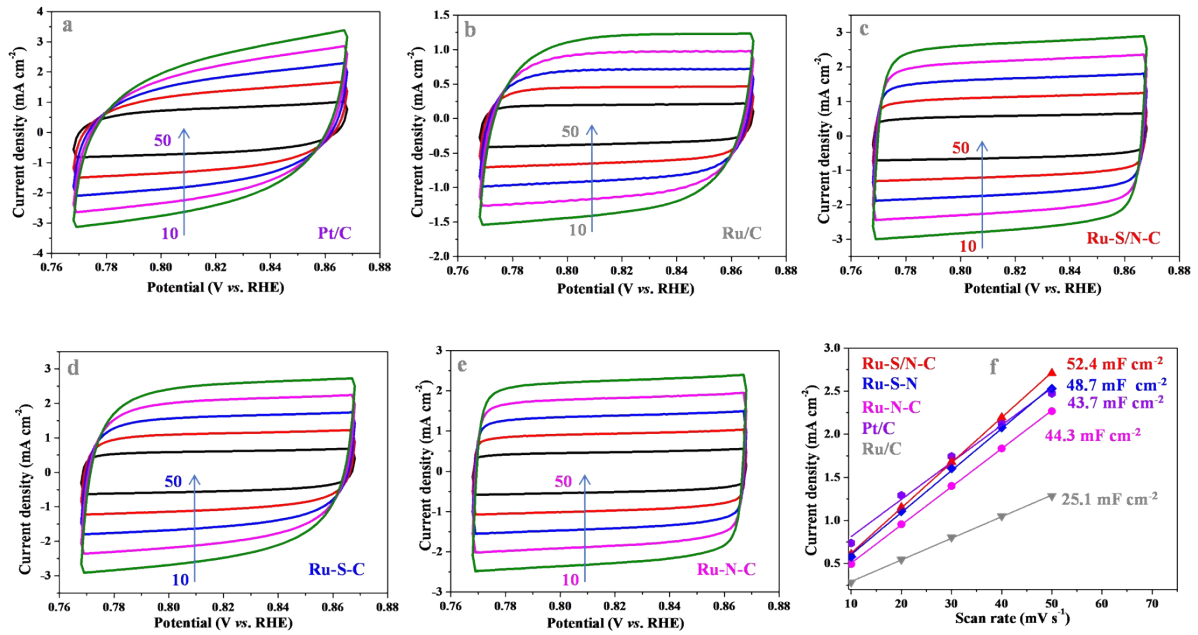**Fig. S14** The Raman spectra of Ru-S/N-C, Ru-N-C and Ru-S-C.

Fig. S15 a-e) cyclic voltammetry curves, and f) current densities at 0.818 V plotted against scan rates for Pt/C, Ru/C, Ru-S/N-C, Ru-S-C and Ru-N-C (Corresponding C_{dl}).
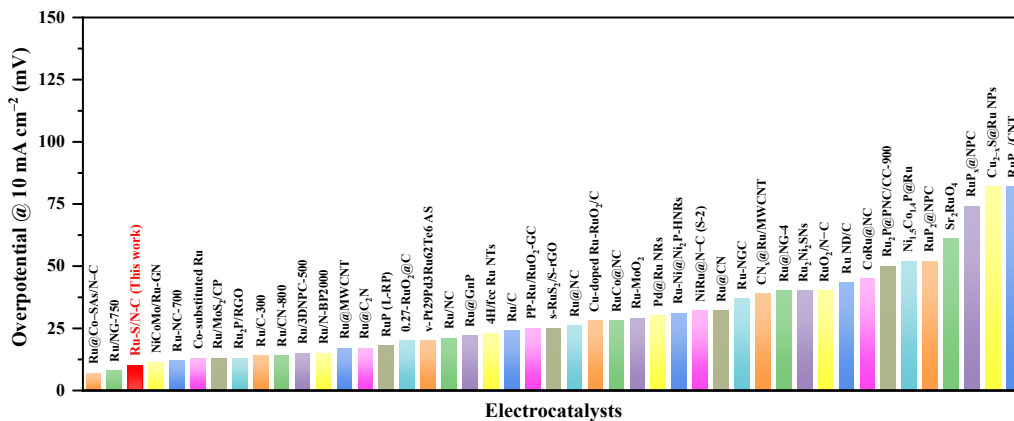

Fig. S16 HER performance comparisons of Ru-S/N-C with those of the reported catalysts.

Table S2. The comparison of the catalytic activity of HER on Ru-S/N-C with the recently reported catalysts in 1.0 M KOH media.

Catalysts	Overpotential (mV @10 mA cm^{-2})	References
Ru@Co–SAs/N–C	7	Nano Energy, 2019, 59, 472–480
Ru/NG-750	8	ACS Appl. Mater. Interfacess, 2017, 9, 3785–3791
Ru-S/N-C	10	This work
NiCoMo/Ru-GN	11.4	J. Phys. Chem. C, 2018, 122, 17621–17631
Ru-NC-700	12	Nat. Commun., 2019, 10, 631
Co-substituted Ru	13	Nat. Commun., 2018, 9, 4958
Ru/MoS$_2$/CP	13	Chem. Commun., 2018, 54, 3343–3346
Ru$_2$P/RGO	13	Chem. Commun., 2018, 54, 3343–3346
Ru/C-300	14	J. Mater. Chem. A, 2018, 6, 14380–14386
Ru/CN-800	14	ACS Sustainable Chem. Eng., 2018, 6, 11487–11492
Ru/3DNPC-500	15	ACS Sustainable Chem. Eng., 2019, 7, 1178–1184
Ru/N-BP2000	15	ChemCatChem 2019, 11, 4327-4333
Ru@C$_2$N	17	Nat. Nanotechnol., 2017, 12, 441–446
RuP (L-RP)	18	Adv. Mater., 30, 2018, 1800047
0.27-RuO$_2$@C	20	Nano Energy, 2019, 55, 49–58
v-Pt$_{29}$Pd$_3$Ru$_{62}$Te$_6$ AS	20	Nano Energy 2019, 61, 346–351
Ru/NC	21	J. Mater. Chem. A, 2017, 5, 25314–25318
Ru@GnP	22	Adv. Mater., 30, 2018, 1803676
4H/fcc Ru NTs	23	Small, 14, 2018,1801090
Ru/C	24	Adv. Energy Mater., 8, 2018, 1801698
PP-Ru/RuO$_2$-GC	25	ACS Catal., 2018, 8, 11094–11102
s-RuS$_2$/S-rGO	25	ACS Appl. Mater. Interfaces, 2018, 10, 34098−34107

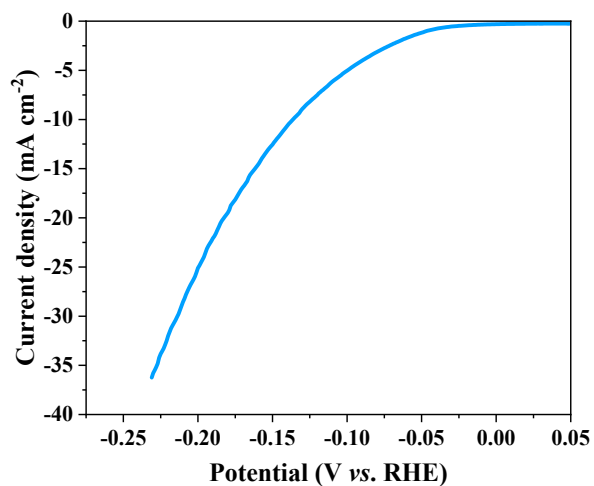|		
Ru@NC	26	Angew. Chem. Int. Ed., 2018, 130, 5950–5954
Cu-doped Ru-RuO$_2$/C	28	Small, 2018, 14, 1803009
RuCo@NC	28	Nat. Commun., 2017, 8, 14969
Ru-MoO$_2$	29	J. Mater. Chem. A, 2017, 5, 5475–5485
Pd@Ru NRs	30	ACS Appl. Mater. Interfaces, 10, 2018, 34147−34152
Ru-Ni@Ni$_2$P-HNRs	31	J. Am. Chem. Soc., 2018, 140, 2731–2734
NiRu@N−C (S-2)	32	J. Mater. Chem., A 2018, 6, 1376−1381
Ru@CN	32	Energy Environ. Sci., 2018, 11, 800–806
Ru-NGC	37	Chem. Commun., 2019, 55, 965–968
CNx@Ru/MWCNT	39	ChemCatChem, 2019, 11, 1970–1976
Ru@NG-4	40	Sustain. Energy Fuels, 2017, 1, 1028−1033
Ru$_2$Ni$_2$ SNs	40	Nano Energy, 2018, 47, 1−7
RuO$_2$/N−C	40	ACS Sustainable Chem. Eng., 2018, 6, 11529− 11535
Ru ND/C	43.4	Chem. Commun., 2018, 54, 4613− 4616
CoRu@NC	45	Nanotechnology, 29, 225403 (2018)
Ru$_2$P@PNC/CC-900	50	ACS Appl. Energy Mater., 2018, 1, 3143–3150
Ni$_{1.5}$Co$_{1.4}$P@Ru	52	Chem. Commun. 2017, 53, 13153–13156
RuP$_2$@NPC	52	Angew. Chem., Int. Ed. 2017, 56, 11559–11564
Sr$_2$RuO4	61	Nat. Commun., 2019, 10, 149
ah-RuO$_2$@C	63	Nano Energy, 2019, 55, 49–58
RuP$_x$@NPC	74	ChemSusChem, 2018, 11, 743–752
Cu$_{2−x}$S@Ru NPs	82	Small, 2017, 13, 1700052
RuP$_2$ /CNT	82	Chemistry, 2019, 25, 8579-8584
RuO$_2$-NWs@g-CN	95	ACS Appl. Mater. Interfaces, 2016, 8, 28678–28688

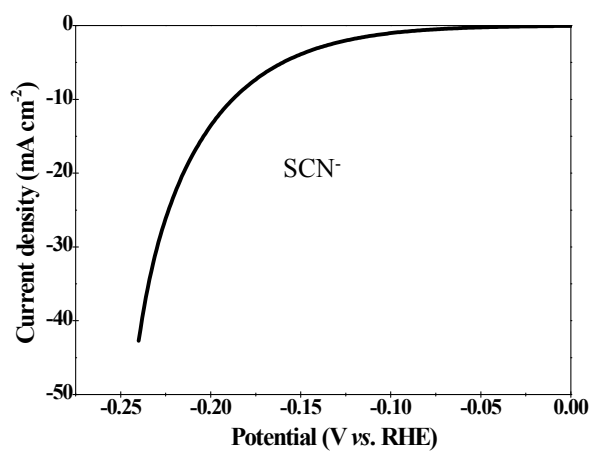**Fig. S17** HER polarization plot of C-N/S in 1.0 M KOH.

Fig. S18 HER polarization plot of Ru-S/N-C with 10 mM KSCN in 1.0 M KOH, indicating that SCN ions strongly poison the active center of Ru-S/N-C catalyst.
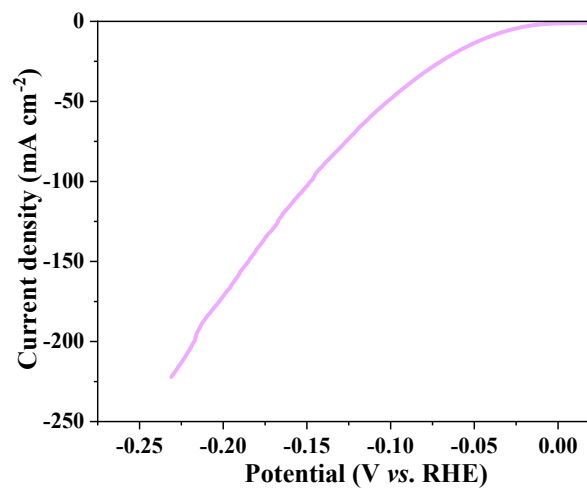
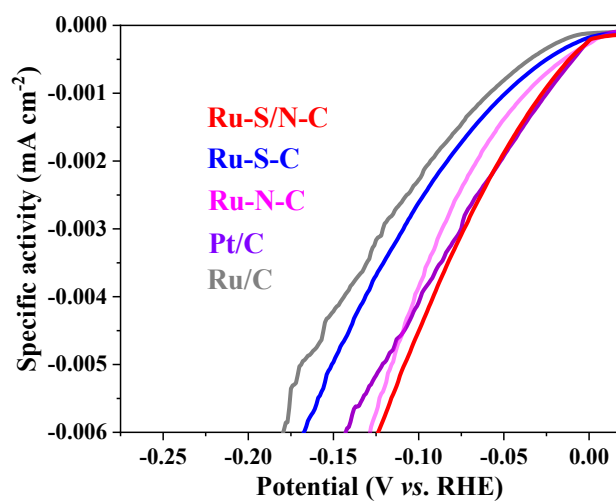**Fig. S19** HER polarization plot of physically mixed Ru/C-S-N in 1.0 M KOH.

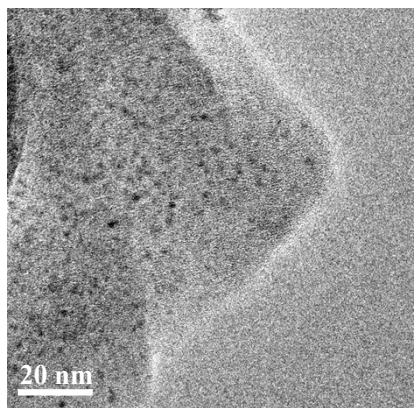**Fig. S20** Comparisons of specific activities of Pt/C, Ru/C, Ru-S/N-C, Ru-S-C and Ru-N-C.

Fig. S21 High-resolution image of Ru-S/N-C after cycling in 1.0 M KOH electrolyte.
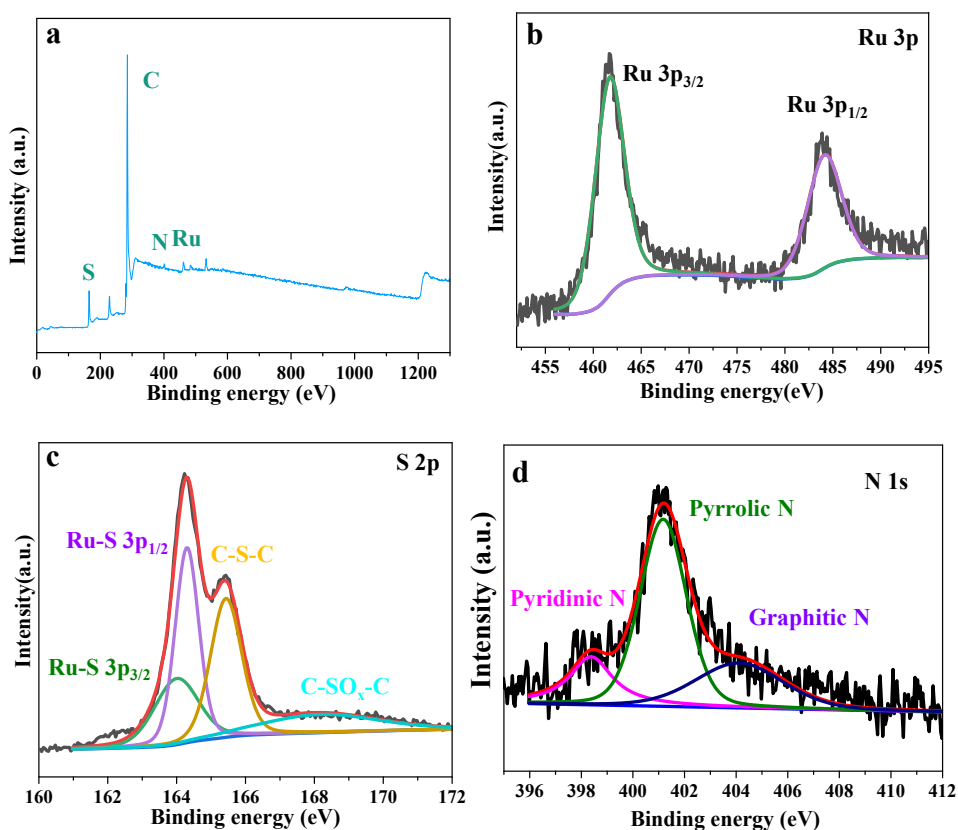

Fig. S22 a**)** XPS survey spectra. High-resolution XPS spectra of b) Ru 3p, c) S 2p and d) N 1s for Ru-S/N-C after cycling.
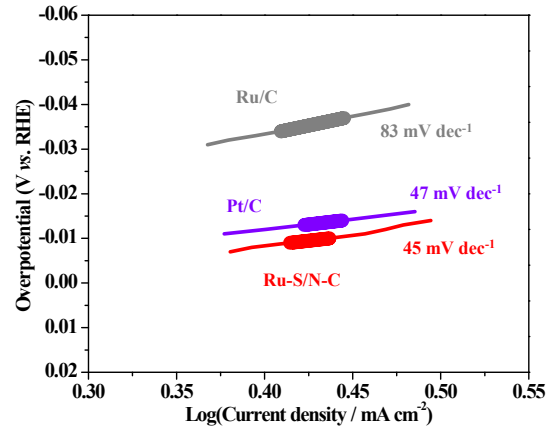
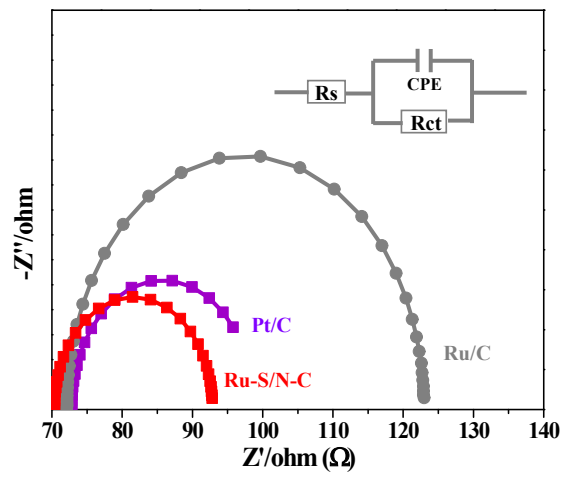**Fig. S23** Tafel plots of Ru-S/N-C, Pt/C and Ru/C

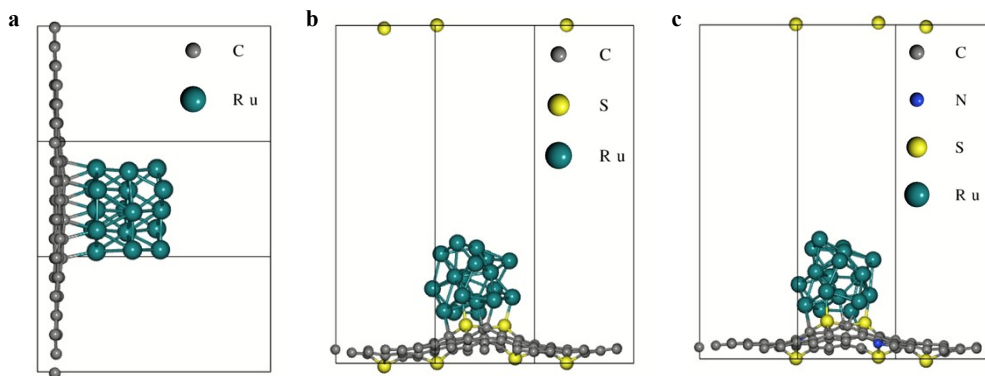**Fig. S24** Nyquist plots for Ru-S/N-C, Pt/C and Ru/C.

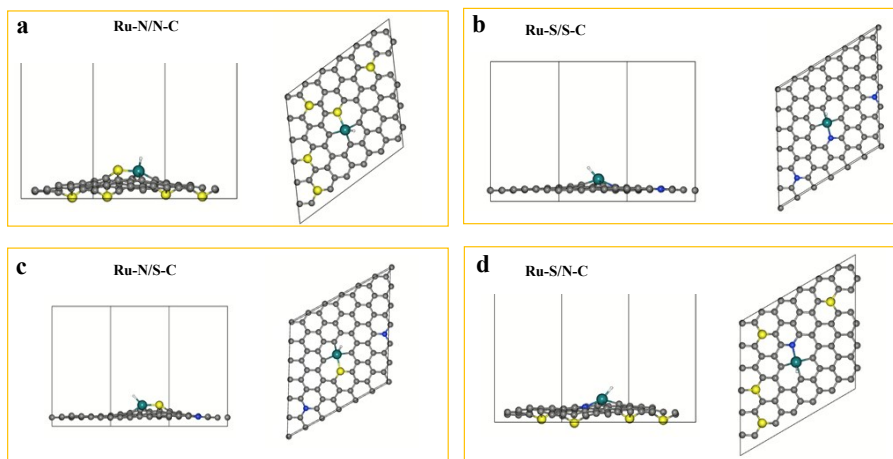**Fig. S25** Theoretical calculated models of Ru/C, Ru/S-C and Ru-S/N-C.

Fig. S26 a-d) Side and top views of theoretical calculated models for Ru$_{single\ atom}$-S/N-C, Ru$_{single\ atom}$-N/N-C, Ru$_{single\ atom}$-N/S-C and Ru$_{single\ atom}$-S/S-C.
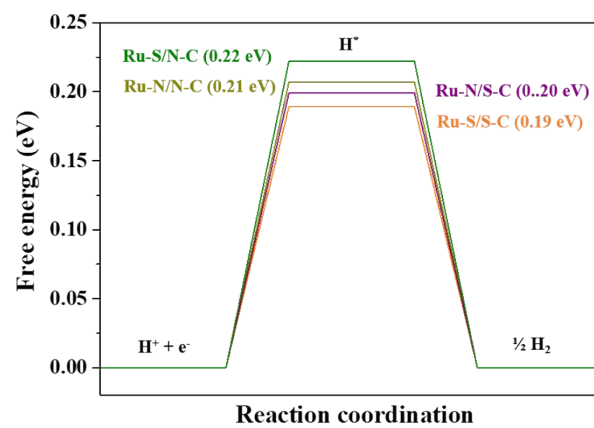
Fig. S27 ΔG_{H*} calculated for hydrogen evolution reaction on various catalysts.